

Computational Study of Core Modified Dipyrriamethyrin for the Competitive Complexation of Am³⁺/Cm³⁺ From Their Trichlorides

Abigail Jennifer G¹, Georg Schreckenbach², and Elumalai Varathan^{1*}

¹Department of Chemistry, SRM Institute of Science and Technology, Kattankulathur, Chennai 603203, Tamil Nadu, India.

²Department of Chemistry, University of Manitoba, Winnipeg, Manitoba, R3T 2N2, Canada.

Email: varathan.elumalai85@gmail.com, varathae@srmist.edu.in

TABLE OF CONTENTS

Table/Figure Number	Table Title	Page Number
Table S1	Cavity size in ligand and complex (in Å).	2
Table S2	NPA charges on the N and O donors of the dipyrriamethyrin and O-substituted ligands after (L1 ²⁻ /L2 ¹⁻ /L3) and before (L1_2H/L2_1H) deprotonation.	2
Table S3	Bond lengths (in Å), bond angles (in °), NPA and Mulliken charges and spin density of the actinide trichloride compounds.	2
Table S4	Calculated Mayer bond orders of the optimized [An(Cl) _m Lm] complexes, m=1,2,3.	3
Table S5	Mulliken charges and spin density on the coordinating atoms of the [An(Cl) _m Lm] complexes (m=1,2,3).	3
Table S6	Electron density (ρ, in e bohr ⁻³) localized on the bond critical points (BCP) of the [An(Cl) _m Lm] complexes, m=1,2,3, based on the QTAIM analysis.	4-5
Table S7	Thermodynamic parameters computed for the formation reaction of actinide chloride-modified dipyrriamethyrin complexes. Energies are given in kcal/mol, where T = 298.15K.	6-7
Figure S1	Various conformers of the protonated dipyrriamethyrin ligand (L1_2H) and modified dipyrriamethyrin (L2_1H) based on the position of the protons along with the total energy of the conformers.	8
Figure S2	Top view (top) and side view (bottom) of the optimized ligands.	9
Figure S3	Optimized geometry of An(Cl) ₃ and [Am(Cl) ₃ (H ₂ O) ₆]	10
Figure S4	QTAIM topology of the complexes.	11

Table S1. Cavity size in ligands and complexes (in Å).

Ligand	N1-N4/O1-N4/O1-O2	N2-N5	N3-N6
L1 ²⁻	5.926	5.923	6.070
L2 ¹⁻	5.956	5.820	5.918
L3	6.061	5.643	5.717

Complex	N1-N4/O1-N4/O1-O2	N2-N5	N3-N6
[Am/Cm(Cl)L1]	5.239/ 5.280	5.255/5.269	5.290/5.358
[Am/Cm(Cl) ₂ L2]	5.775/5.790	5.392/5.401	5.509/5.507
[Am/Cm(Cl) ₃ L3]	6.009/5.991	5.444/5.326	5.444/5.412

Table S2. NPA charges on the N and O donors of the dipyrimythyridin and O-substituted ligands after (L1²⁻/L2¹⁻/L3) and before (L1_2H/L2_1H) deprotonation.

Ligand	N1/O1	N2	N3	N4/O2	N5	N6
L1 ²⁻	-0.372	-0.375	-0.315	-0.372	-0.375	-0.322
L2 ¹⁻	-0.312	-0.374	-0.326	-0.382	-0.371	-0.335
L3	-0.310	-0.386	-0.341	-0.312	-0.385	-0.346
L1_2H	-0.433	-0.461	-0.378	-0.436	-0.459	-0.381
L2_1H	-0.313	-0.435	-0.354	-0.393	-0.450	-0.371

Table S3. Bond lengths (in Å), bond angles (in °), bond orders, NPA and Mulliken charges and spin densities of the actinide trichloride compounds.

Compound	Bond length	Bond angles	Mayer bond order	NPA charge		NPA spin density		Mulliken charge		Mulliken spin density	
				An	Cl	An	Cl	An	Cl	An	Cl
AmCl ₃	2.523	117.4	1.093	1.510	-0.503	6.219	-0.073	1.116	-0.372	6.253	-0.084
CmCl ₃	2.508	118.1	1.081	1.620	-0.540	6.905	0.031	1.164	-0.388	6.953	0.021

Table S4. Calculated Mayer bond orders of the optimized $[\text{An}(\text{Cl})_m\text{L}_m]$ complexes, $m=1,2,3$.

Complex	An-N1/O1	An-N2	An-N3	An-N4/O2	An-N5	An-N6	An-Cl1	An-Cl2	An-Cl3
$[\text{Am}(\text{Cl})\text{L1}]$	0.302	0.302	0.261	0.294	0.308	0.256	0.890		
$[\text{Am}(\text{Cl})_2\text{L2}]$	0.058	0.284	0.134	0.213	0.297	0.175	0.823	0.812	
$[\text{Am}(\text{Cl})_3\text{L3}]$	0.077	0.214	0.162	0.075	0.221	0.147	0.746	0.768	0.774
$[\text{Cm}(\text{Cl})\text{L1}]$	0.277	0.288	0.229	0.278	0.286	0.236	0.944		
$[\text{Cm}(\text{Cl})_2\text{L2}]$	0.052	0.292	0.128	0.214	0.312	0.162	0.778	0.777	
$[\text{Cm}(\text{Cl})_3\text{L3}]$	0.072	0.205	0.147	0.069	0.209	0.136	0.680	0.736	0.747

Table S5. Mulliken charges and spin density on the coordinating atoms of the $[\text{An}(\text{Cl})_m\text{L}_m]$ complexes ($m=1,2,3$).

Complex	An	N1/O1	N2	N3	N4/O2	N5	N6	Cl1	Cl2	Cl3
Mulliken charges (Q)										
$[\text{Am}(\text{Cl})\text{L1}]$	1.504	-0.485	-0.489	-0.435	-0.484	-0.490	-0.437	-0.453		
$[\text{Am}(\text{Cl})_2\text{L2}]$	1.423	-0.503	-0.449	-0.505	-0.405	-0.441	-0.508	-0.474	-0.478	
$[\text{Am}(\text{Cl})_3\text{L3}]$	1.235	-0.495	-0.465	-0.385	-0.491	-0.472	-0.383	-0.503	-0.475	-0.473
$[\text{Cm}(\text{Cl})\text{L1}]$	1.568	-0.491	-0.497	-0.437	-0.491	-0.499	-0.438	-0.424		
$[\text{Cm}(\text{Cl})_2\text{L2}]$	1.460	-0.493	-0.514	-0.398	-0.457	-0.525	-0.430	-0.504	-0.506	
$[\text{Cm}(\text{Cl})_3\text{L3}]$	1.262	-0.494	-0.470	-0.377	-0.490	-0.475	-0.375	-0.538	-0.499	-0.495
Mulliken spin density										
$[\text{Am}(\text{Cl})\text{L1}]$	6.1883	-0.0376	-0.0337	-0.0285	-0.0327	-0.0386	-0.0274	-0.0203		
$[\text{Am}(\text{Cl})_2\text{L2}]$	6.1249	-0.0008	-0.0127	-0.0190	-0.0008	-0.0087	-0.0192	-0.0569	-0.0556	
$[\text{Am}(\text{Cl})_3\text{L3}]$	6.0890	-0.0009	-0.0179	0.0002	-0.0007	-0.0190	0.0009	-0.0545	-0.0483	-0.0468
$[\text{Cm}(\text{Cl})\text{L1}]$	6.9891	-0.0038	-0.0040	-0.0013	-0.0041	-0.0045	-0.0011	-0.0018		
$[\text{Cm}(\text{Cl})_2\text{L2}]$	6.9656	-0.0007	-0.0103	-0.0028	-0.0060	-0.0129	-0.0039	0.0186	0.0182	
$[\text{Cm}(\text{Cl})_3\text{L3}]$	6.9508	-0.0011	-0.0071	-0.0023	-0.0010	-0.0074	-0.0021	0.0173	0.0137	0.0137

Table S6. Electron density (ρ , in $e \text{ bohr}^{-3}$) localized on the bond critical points (BCP) of the $[\text{An}(\text{Cl})_m\text{L}_m]$ complexes, $m=1,2,3$, based on the QTAIM analysis.

Complex	ρ at BCPs of An-N/O bonded interactions						ρ at BCPs of An-Cl bonds			ρ at BCPs of non-bonded interactions			
	An-N1/O1	An-N2	An-N3	An-N4/O2	An-N5	An-N6	An-Cl1	An-Cl2	An-Cl3	O1-N1	O1-Cl2	O2-N5	O2-Cl3
[Am(Cl)L1]	0.0406	0.0411	0.0377	0.0416	0.0396	0.0369	0.0716	-	-	-	-	-	-
[Am(Cl) ₂ L2]	0.0083	0.0258	0.0382	0.0519	0.0484	0.0209	0.0640	0.0634	-	0.0083	-	-	-
[Am(Cl) ₃ L3]	0.0119	0.0368	0.0247	0.0112	0.0382	0.0265	0.0570	0.0594	0.0595	0.0090	0.0125	0.0122	0.0087
[Cm(Cl)L1]	0.0384	0.0401	0.0356	0.0397	0.0380	0.0344	0.0762	-	-	-	-	-	-
[Cm(Cl) ₂ L2]	0.0071	0.0236	0.0378	0.0540	0.0497	0.0200	0.0628	0.0638	-	0.0083	-	-	-
[Cm(Cl) ₃ L3]	0.0108	0.0377	0.0252	0.0115	0.0370	0.0240	0.0588	0.0549	0.0588	0.0090	0.0124	0.0126	0.0093

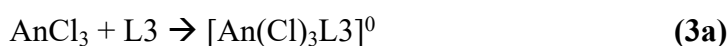
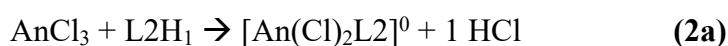
Bader's QTAIM analysis was carried out and the electron density (ρ) at the bond critical points (BCPs) were computed as shown in **Table S6**. The QTAIM topology is shown in **Figure S4**. It is known that ionic and covalent interactions are characterised with $\rho < 0.1 \text{ e/bohr}^3$ and $\rho > 0.2 \text{ e/bohr}^3$, respectively.^{1,2} From the table it is evident that all the interactions are ionic in nature. Generally, the ρ at the BCP of An-N3 and An-N6 bonds are smaller compared to other bonds, and the density ρ at the BCP of An-Cl is the highest. This confirms that the pyridine nitrogen atoms N3 and N6 contribute less than the other N atoms to the bonding interaction of the ligand with the An, and the Cl atoms are binding more strongly than the L1²⁻ donor atoms. In L2 based complexes, the ρ of the An-O1 bond is the least while those of the An-N BCPs are high, confirming that the An shifts far from the O atom in the ligand cavity. This observation is in line with the discussions of the bond lengths and bond orders, *vide supra*. Further, O1 exhibits non-bonded interaction with N2. This can be accounted for by the slight shift of the An closer to N4, N5, as observed from the bond lengths, due to the decrease in the contribution of N2 as a result of its non-covalent interaction with the adjacent O atom. In the L3 based complexes, ρ increases in the order: An-O1/2 < An-N3/N6 < An-N2/N5 < An-Cl. Further, O1 and O2 interact non-covalently with the Cl atoms (of the same plane) due to the adjacent position of the atoms in the complex. The symmetric nature of the L3 based complexes may lead to better bonding compared to the unsymmetric O substituted L2¹⁻ based complexes, given the multiple BCPs observed in the former compared to the latter. This conclusion is supported by the observation made in the discussion on bond lengths.

Reference:

- 1) Brewster, J. T.; Mangel, D. N.; Gaunt, A. J.; Saunders, D. P.; Zafar, H.; Lynch, V. M.; Boreen, M. A.; Garner, M. E.; Goodwin, C. A. P.; Settineri, N. S.; Arnold, J.; Sessler, J. L. In-Plane Thorium(IV), Uranium(IV), and Neptunium(IV) Expanded Porphyrin Complexes. *J Am Chem Soc* 2019, 141 (44), 17867–17874. <https://doi.org/10.1021/jacs.9b09123>.
- 2) Yang, M.; Ding, W.; Wang, D. Characterization of the Binding of Six Actinyls AnO₂^{2+/+} (An = U/Np/Pu) with Three Expanded Porphyrins by Density Functional Theory. *New Journal of Chemistry* 2017, 41 (1), 63–74. <https://doi.org/10.1039/C6NJ01615D>.

Table S7. Thermodynamic parameters computed for the formation reaction of actinide chloride-modified dipyrriamethyrin complexes. Energies are given in kcal/mol, where T = 298.15K.

Complex formation reactions							
	Am	Cm	Am	Cm	Am	Cm	
	Eq. (1a) ...gas		Eq. (2a) ...gas		Eq. (3a) ...gas		
ΔG	-16.04	-14.98	-43.00	-44.86	-44.90	-46.71	
$\Delta\Delta G_{Am/Cm}$		-1.06		1.86		1.81	
ΔH	-10.46	-9.15	-47.12	-48.80	-59.54	-61.15	
ΔE	-6.12	-4.86	-46.47	-48.32	-62.60	-64.32	
$-T\Delta S$	-5.57	-5.83	4.12	3.93	14.64	14.44	
	Eq. (1a) ...DCM		Eq. (2a) ...DCM		Eq. (3a) ...DCM		
ΔG	9.07	10.29	-16.68	-20.13	-24.27	-27.46	
$\Delta\Delta G_{Am/Cm}$		-1.22		3.45		3.19	
ΔH	14.41	15.30	-20.65	-24.60	-38.37	-42.11	
ΔE	18.69	19.52	-20.12	-24.18	-41.50	-45.28	
$-T\Delta S$	-5.33	-5.00	3.96	4.46	14.09	14.64	



The energetics associated with reactions (1a), (2a) and (3a) were analysed in both gas and DCM medium. In gaseous phase, 1a is spontaneous for both Am and Cm complexes, where the highly negative Gibbs free energy (ΔG) value suggest more spontaneity to form the $[\text{Am}(\text{Cl})\text{L1}]$ over the $[\text{Cm}(\text{Cl})\text{L1}]$ complex. From (2a) and (3a), we can observe that the formation is spontaneous only at low temperatures. However, the slightly more negative ΔG for formation of $[\text{Cm}(\text{Cl})_2\text{L2}]$ (-44.86 kcal/mol) and $[\text{Cm}(\text{Cl})_3\text{L3}]$ (-46.71 kcal/mol) than for corresponding Am complexes indicates favoured complexation of Cm over Am by O-substituted ligands. This supports the observation made in the bond parameters where Cm complexes were characterized with shorter Cm-O1/2 bond lengths than Am-O1/2. The $\Delta\Delta G_{Am/Cm}$ (i.e., $\Delta\Delta G_{Am/Cm} = [\Delta G \text{ of Am complex} - \Delta G \text{ of Cm complex}]$) values confirm that the O substituted ligands prefer the Cm based complexes over Am complexes. Complementing the observations in the bond parameters and charges, the optimum 4N:2O ratio in L3 shows a noticeable difference in the energetics compared to L2¹⁻, where the absolute ΔG values become more negative indicating higher spontaneity, while high positive $-T\Delta S$ values indicate the reaction to occur at a lower temperature in the former than the latter.

In the solvent medium, reaction (1a) would be spontaneous only at elevated temperatures, while (2a) and (3a) suggest the formation to be feasible at lower temperatures. Cm complexation with L2¹⁻ and L3 is favoured compared to Am, as observed in gas phase supporting the previously

discussed geometric and electronic properties. We can also suggest that a substitution of O donor atom into the dipyrriamethyrin alters the ligand affinity towards the heavier actinide, while the optimum ratio could be either 5N:1O (in L2¹⁻) or 4N:2O (in L3), given the marginal difference in the formation energies, and this is confirmed by the $\Delta\Delta G_{Am/Cm}$. The overall trend observed among the energy parameters computed in the DCM solvent medium are comparable to those calculated in the gas-phase.

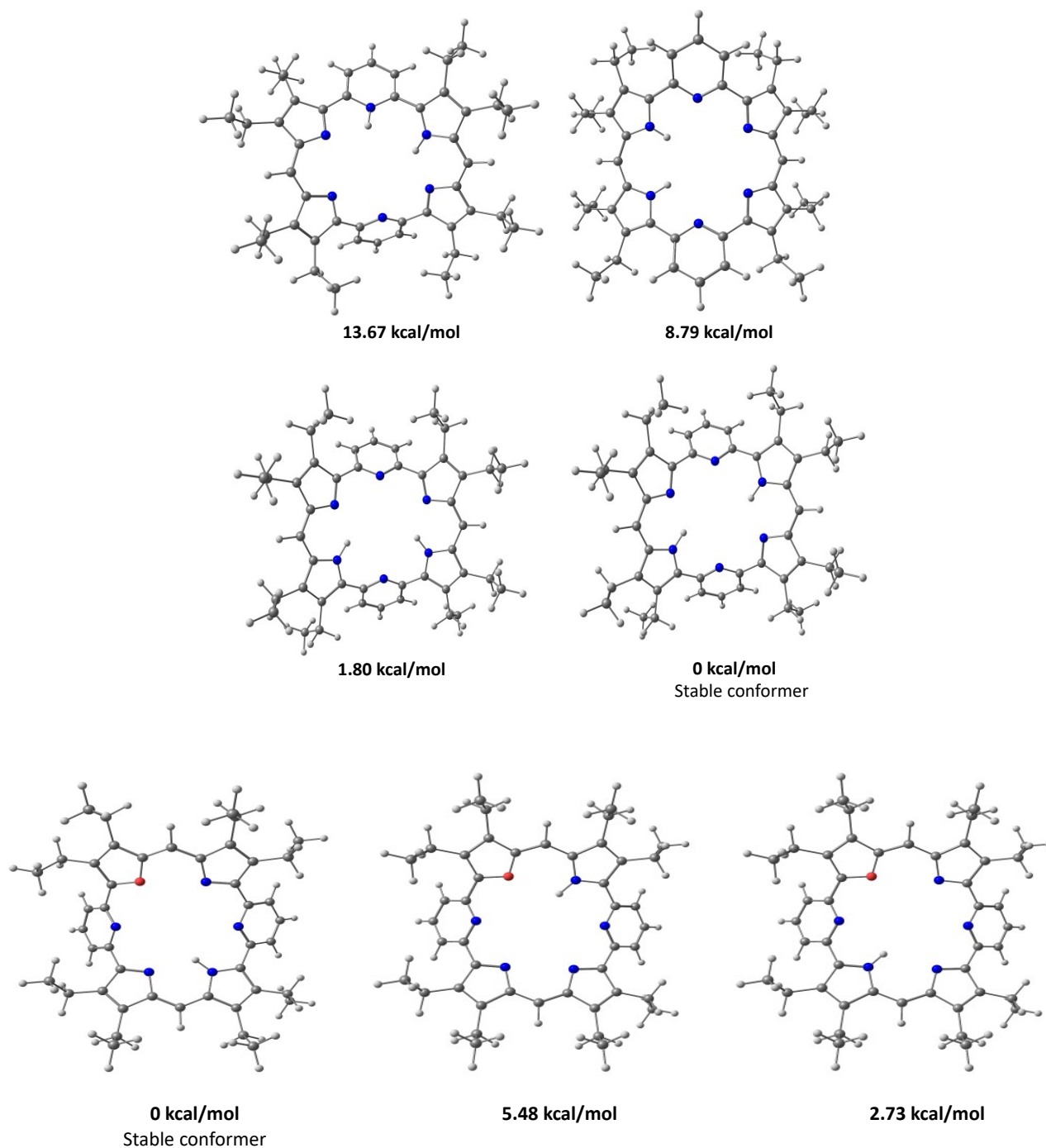


Figure S1. Various conformers of the protonated dipyriamethyrin ligand (L1_2H, top) and modified dipyriamethyrin (L2_1H, bottom row) based on the position of the protons along with the relative energies of the conformers. Grey - carbon, white – hydrogen, blue – nitrogen and red – oxygen.

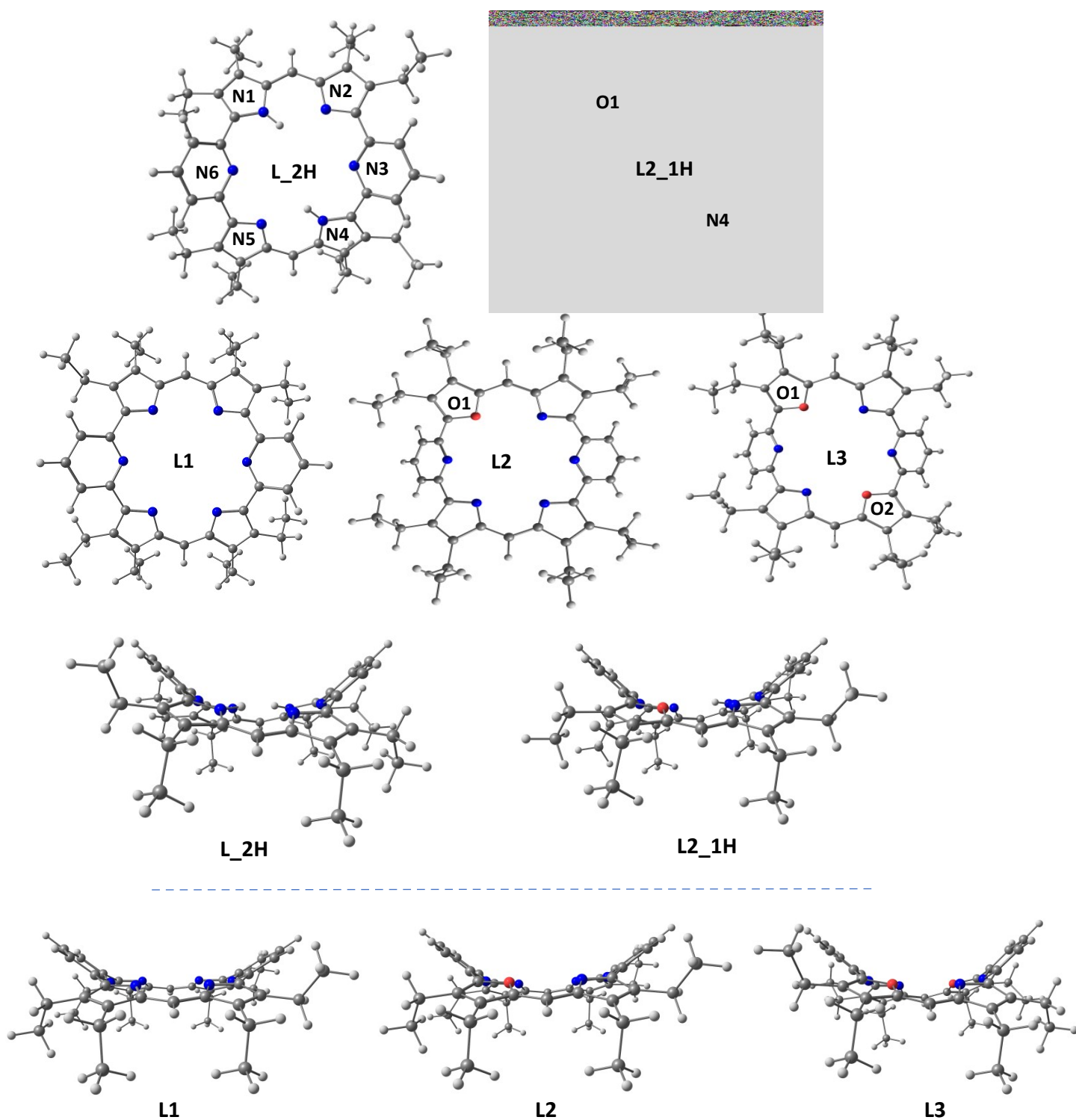


Figure S2. Top view (top) and side view (bottom) of the optimized ligands

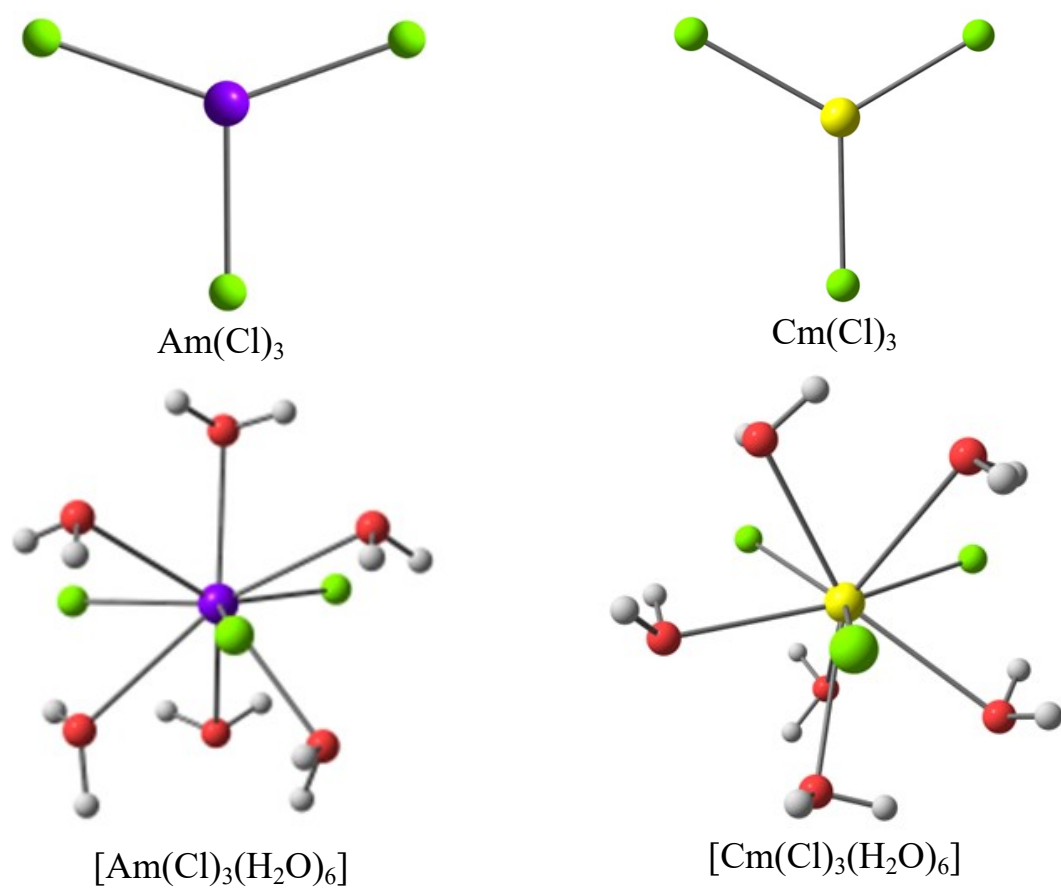


Figure S3. Optimized geometries of $\text{Am}(\text{Cl})_3$ and $[\text{Am}(\text{Cl})_3(\text{H}_2\text{O})_6]$

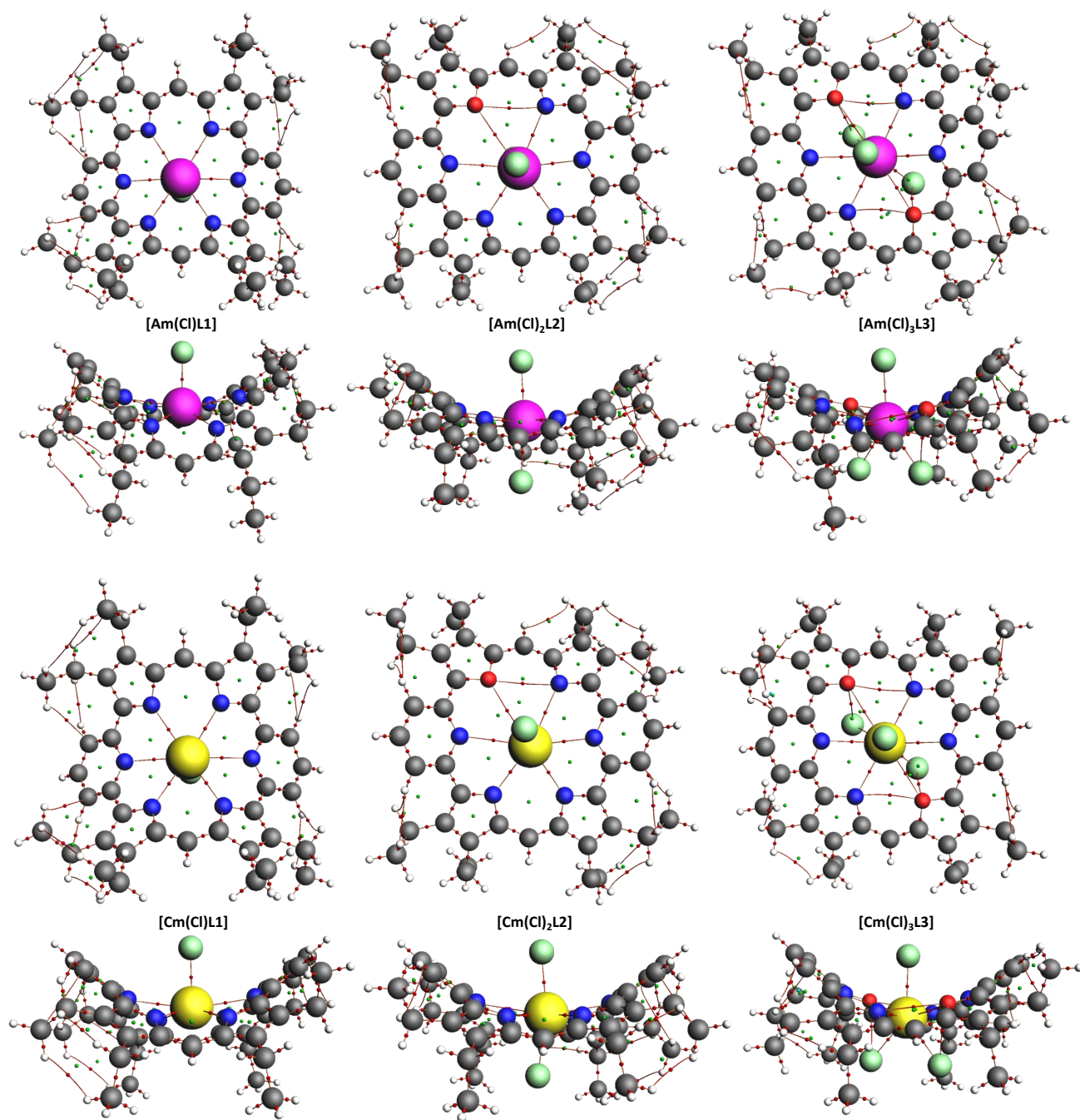


Figure S4. QTAIM topology of the complexes.